Microscopic Description of Nuclear Fission:

Induced fission of ^{240}Pu in real time

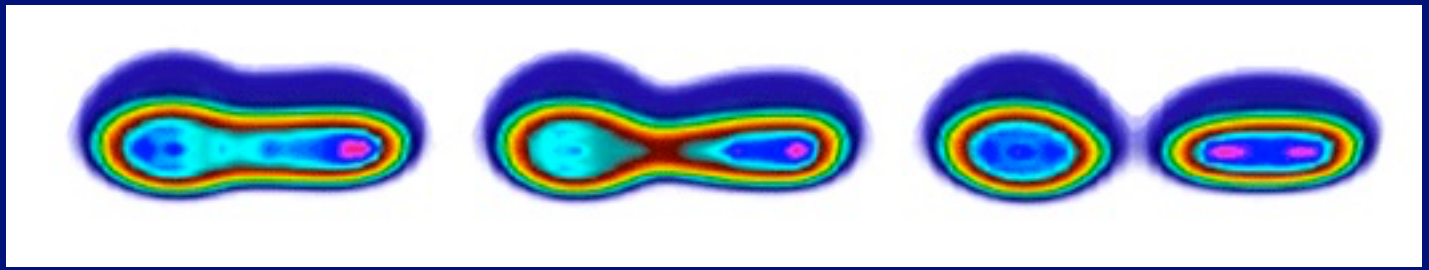

Aurel Bulgac
University of Washington

Collaborators: **Piotr Magierski** **(Warsaw UT and UoW)**
Kenneth J. Roche **(PNNL and UoW)**
Ionel Stetcu **(Theory Division, LANL)**

Slides (pptx) with movies will be available for download from
http://www.faculty.washington.edu/bulgac/Pu240/

Nuclear fission is unquestionably one of the most challenging quantum many-body problems.

Important for fundamental nuclear theory, origin of elements, applications.

Several recent developments have changed radically our prospects of attaining a microscopic description of fission, almost 80 years after it was experimentally discovered.

(In comparison superconductivity needed less than 50 years to attain this goal, from 1911 to 1957.)

- **Formulation of a local extension of the Density Functional Theory (DFT), in the spirit of the Local Density Approximation (LDA) formulation of DFT due to Kohn and Sham, to superfluid time-dependent phenomena, the Superfluid Local Density Approximation (SLDA).**

- **Validation and verification of (TD)SLDA against a large set of theoretical and experimental data.**

- **Emergence of very powerful computational resources.**

- **Non-trivial numerical implementation of SLDA and Time-Dependent SLDA (TDSLDA) and deployment of complex codes using the most advanced capabilities of leadership class computers, in particular taking advantage of tens of thousands of GPUs.**

SLDA and TDSLDA are problems of extreme computational complexity, requiring the solution of 10,000 … 1,000,000 coupled complex non-linear time-dependent 3D partial differential equations.

This presentation is a perfect illustration of Dave Barry's suggestion:

Never be afraid to try something new. Remember that amateurs built the Ark and professionals built the Titanic.

I definitely could not call myself a fission or high-performance computing expert at the time when this project started around 2006. At that time nuclear fission looked to me like a good problem to give it a try, being unaware of how complex really is and not having someone around to warn me.

Now I know a bit more.

But then again, as Sydney Brenner (Nobel prize 2002) said:

I'm a strong believer that ignorance is important in science. If you know too much, you start seeing why things won't work. That is why it's important to change your field to collect more ignorance.

Potential energy versus deformation

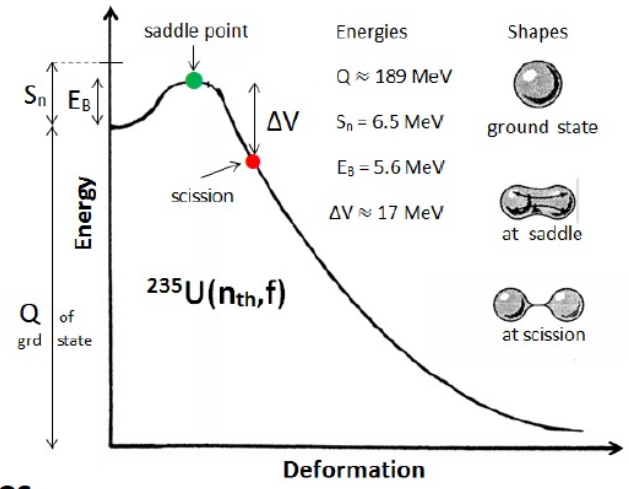

Times

- Time from grd state to saddle in low energy fi $6 \cdot 10^{-15}$ s
- Time from saddle to scission ≈ 5 zs
- Neck rupture in ≈ 0.5 zs
- Acceleration of FF to 90% of final velocity ≈ 5 *zs*
- Time for relaxation of deformation ≈ 5 zs
- Evaporation time for 10 MeV n from FF 10^3 zs

NOTE: 1 zs = 1 zeptosecond = 10^-21 s

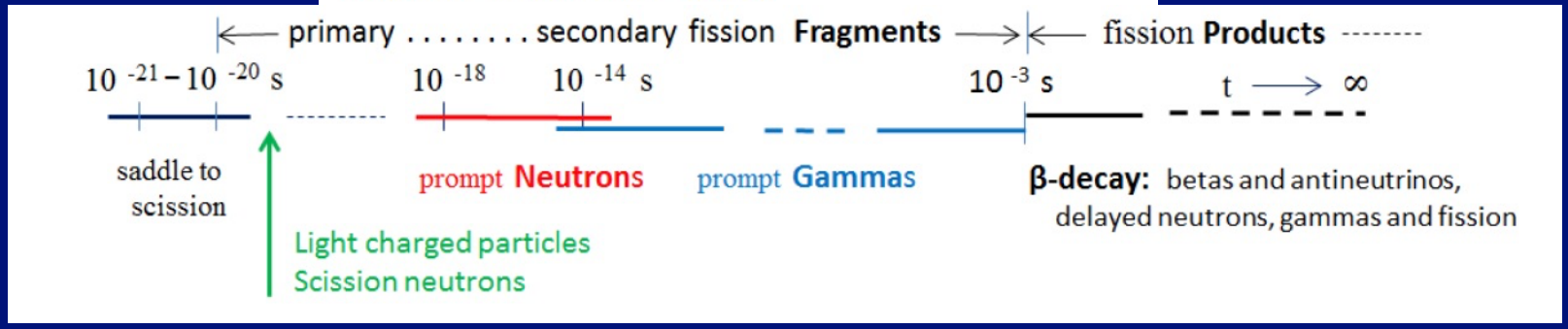

From Lectures given by Gönnenwein at LANL Fiesta School, 2014

How nuclei change their shape at a microscopic level?

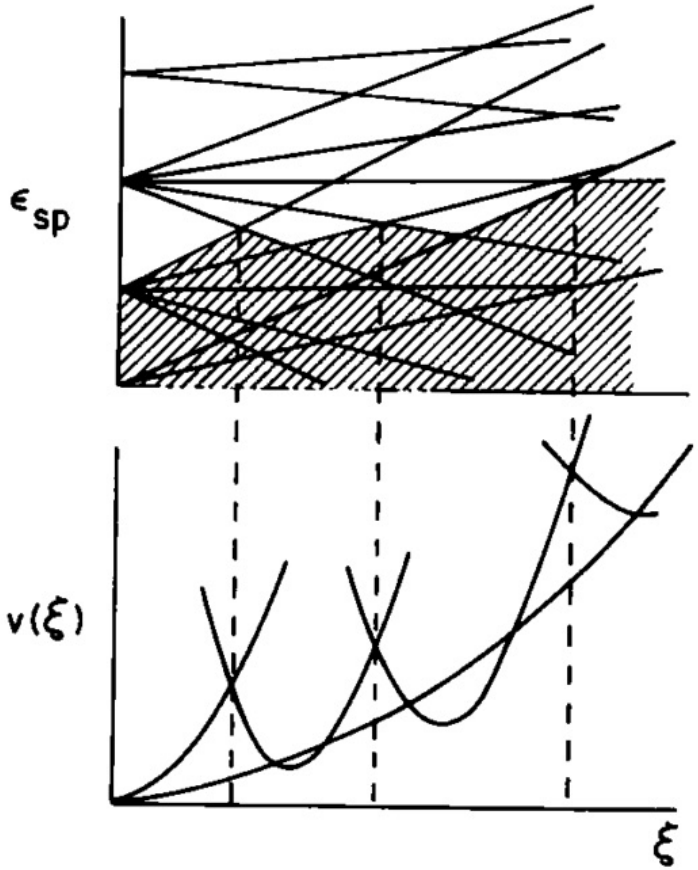

- While a nucleus elongates, the Fermi surface becomes oblate. Its sphericity can be restored only by redistributing the nucleons on different energy levels.

- Each single-particle level double is occupied with time-reversed quantum numbers (in the shaded area)
- At each crossing two nucleons change their angular momenta (m,-m) => (m',-m')
  "Cooper pair" => "Cooper pair"

- <u>Pairing interaction/superfluidity is the most effective mechanism at performing such transitions</u>

From Barranco, Bertsch, Broglia, and Vigezzi
Nucl. Phys. A512, 253 (1990)

Let us consider an axially symmetric nucleus, with Oz the axis of symmetry and evaluate semiclassically the angular momentum distribution

$$P(m) = \int d^3r d^3p\, f(\vec{p},\vec{r})\,\delta\left((\vec{r}\times\vec{p})_z - m\right) = \frac{A^{2/3}}{p_F r_0}\, g\left(\frac{l_z}{p_F r_0 A^{1/3}}\right)$$

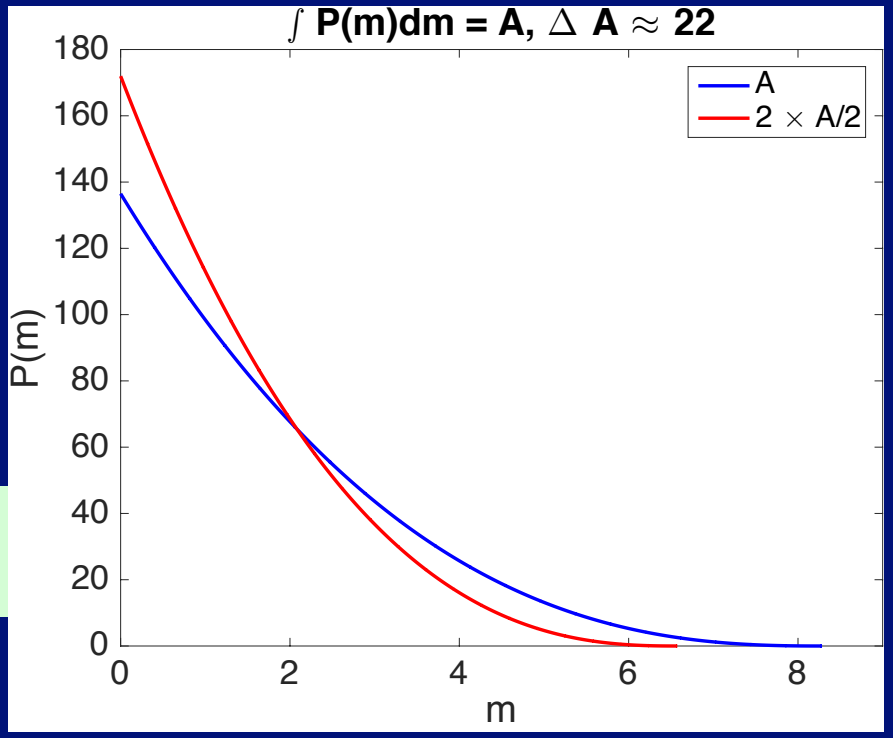

Distribution derived by G.F. Bertsch

However, in TDHF or TDHF with frozen occupation probabilities $P(l_z)$ is conserved.

Single-particle states with $|l_z| \approx O(k_F r_0 A^{1/3})$, which should not be occupied in the fission fragments, retain their initial occupation probability.

Thus, the initial spherical Fermi momentum distribution acquires an ellipsoidal prolate shape in the final fission fragments.

Bertsch and Bulgac, Phys. Rev. Lett. 79, 3539 (1997)

A different mechanism for nuclear shape evolution was advocated by

J.W. Negele, Nucl. Phys. A 502, 371c-386c (1989)
Microscopic theory of fission dynamics

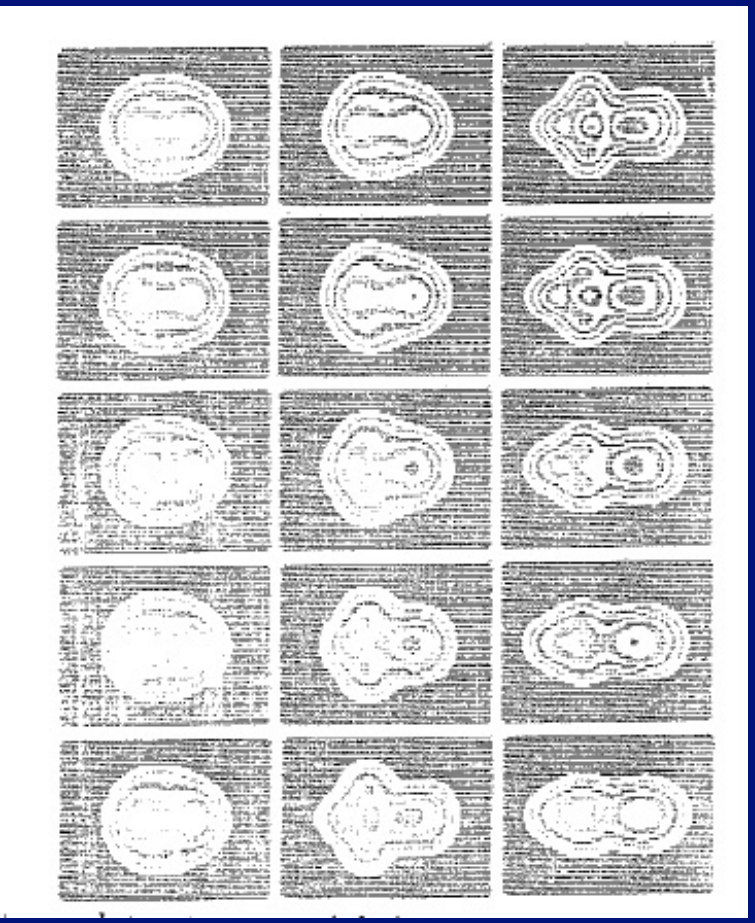

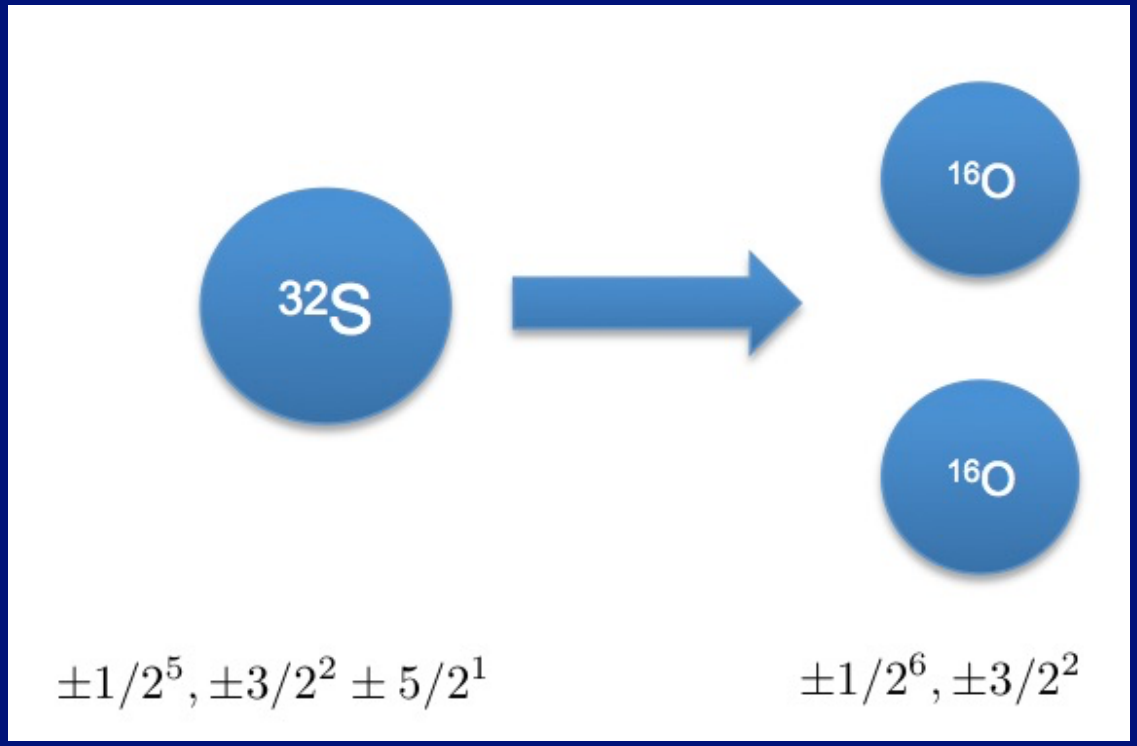

Occupied sp orbitals m-quantum numbers in initial and final configurations

One more problem!
Initial nucleus: 20 positive + 12 negative parity sp orbitals
Final nuclei: 16 positive + 16 negative parity sp orbitals

TDHF + BCS with constant pairing gap

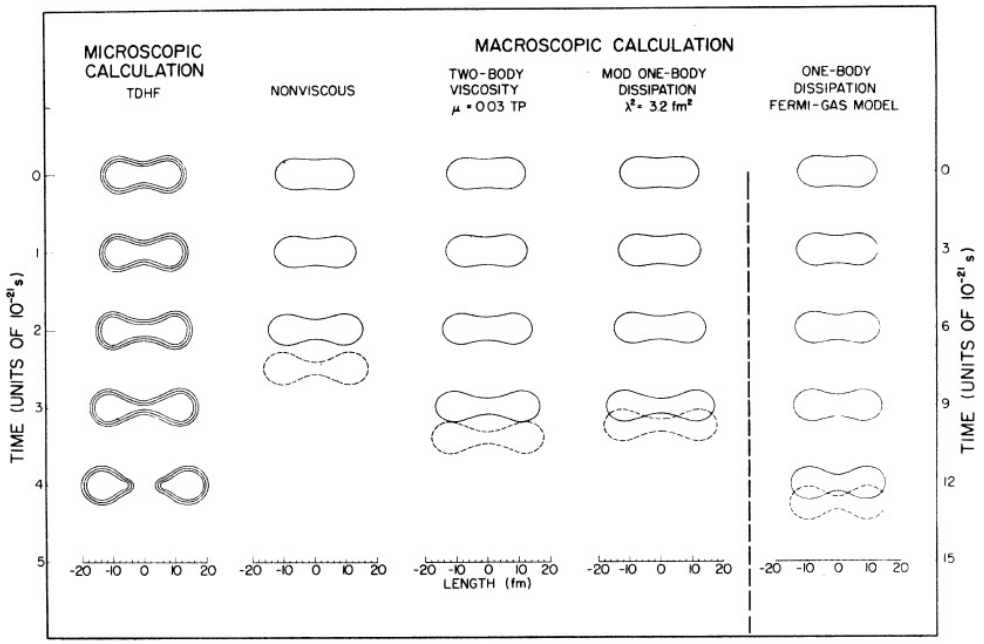

FIG. 6. Comparison as a function of time of shapes for ^{236}U with zero spin-orbit interaction calculated in the TDHF approximation for $\Delta = 2$ MeV and in a macroscopic approach with various types of dissipation. For modified one-body dissipation, we show the result for the preliminary value of $\lambda^2 = 3.2$ fm^2; the final value is 3 fm^2 (Ref. 36). Note that the time scale for the original one-body dissipation is 3 times as long as the time scale for the remaining cases.

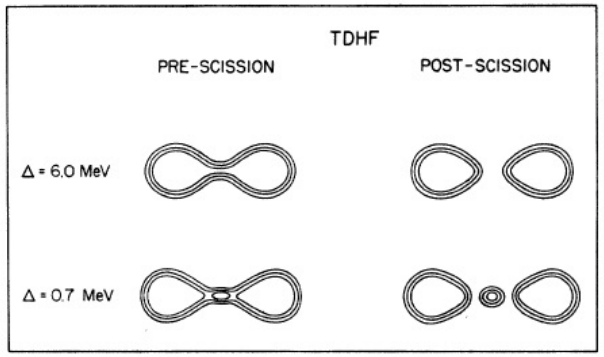

FIG. 7. Comparison of prescission and postscission shapes for ^{236}U with zero spin-orbit interaction calculated in the TDHF approximation for two values of the effective pairing gap Δ. The elapsed time between the two configurations for each Δ is 0.4×10^{-21} s.

TABLE III. Comparison of experimental and calculated most probable fission-fragment kinetic energies for the fission of the compound nucleus ^{236}U. The initial conditions for each calculation correspond to starting from rest 1 MeV beyond the fission saddle point.

Result	Kinetic energy (MeV)
Experimental[a]	168.0 ± 4.5
Microscopic	
$\Delta = 6$ MeV	166
$\Delta = 2$ MeV	142
Macroscopic	
Nonviscous	186
Two-body viscosity, $\mu = 0.03$ TP	167
Modified one-body dissipation, $\lambda^2 = 3$ fm^2	166
One-body dissipation, Fermi-gas value	177

[a] For the fission of ^{232}Th induced by 65.0 MeV α particles, averaged over all fission-fragment mass divisions and corrected for the effects of fragment neutron emission (Ref. 64).

From Negele, Koonin, Möller, Nix, and Sierk
Phys. Rev. C 17, 1098 (1978)

- **Can the adoption of a TDHF + TDBCS approach to fission help restore the sphericity of the Fermi sphere in the fission fragments?**

- **A little bit.**

  - **In TDHF the nucleus is allowed to acquire in principle any shape, but whether dynamically that is realized is not a foregone conclusion.**

  - **Adding TDBCS to TDHF adds one "complex" collective degree of freedom to the many shape degrees of freedom, a spatially constant throughout the entire space complex time dependent pairing field $\Delta(t)$.**

  - **The phase of $\Delta(t)$ can be eliminated with a trivial gauge transformation, which leads to a small renormalization of the chemical potential, leaving effectively only one additional collective degree of freedom when compared to TDHF, namely $|\Delta(t)|$. Thus TDHF+TDBCS amounts to adding practically only one additional collective degree of freedom.**

  - **Practice shows that nuclei cannot always fission within TDHF + TDBCS. This is likely related to the fact that the initial spherical Fermi surface cannot evolve into two spherical Fermi surfaces in the fission fragments within TDHF + TDBCS.**

  - **Continuity equation is violated in a TDHF + TDBCS approach.**

TDHF +TDBCS

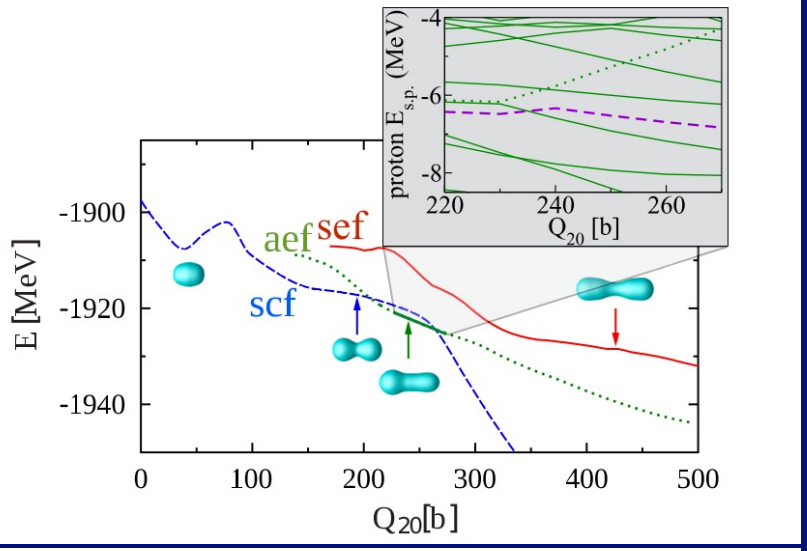

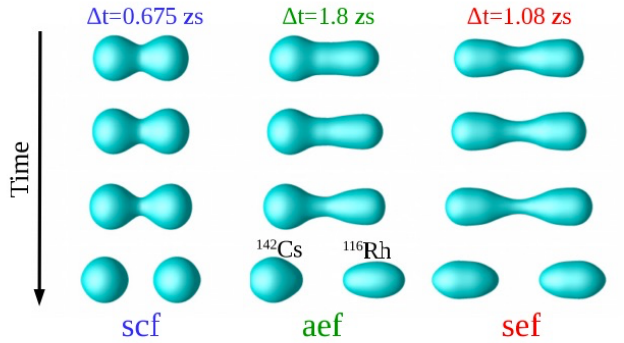

FIG. 2. (Color online) Isodensity surfaces at half the saturation density $\rho_0/2 = 0.08$ fm^{-3} as a function of time for the three modes. The time steps between two images Δt are given at the top of the figure.

From Scamps, Simenel, and Lacroix,
Phys. Rev. C 92, 011602 (2015)

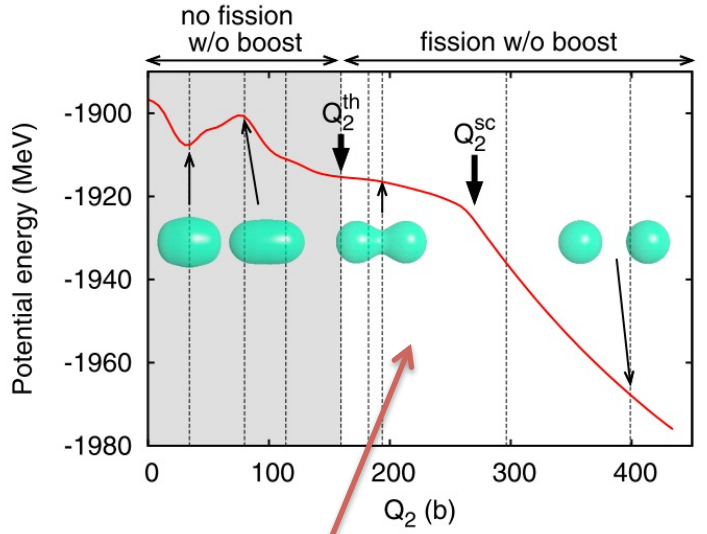

FIG. 1. (Color online) Potential energy curve of ^{258}Fm nucleus as a function of the quadrupole deformation parameter (in barn units).

In this region the Fermi surface is already spherical.

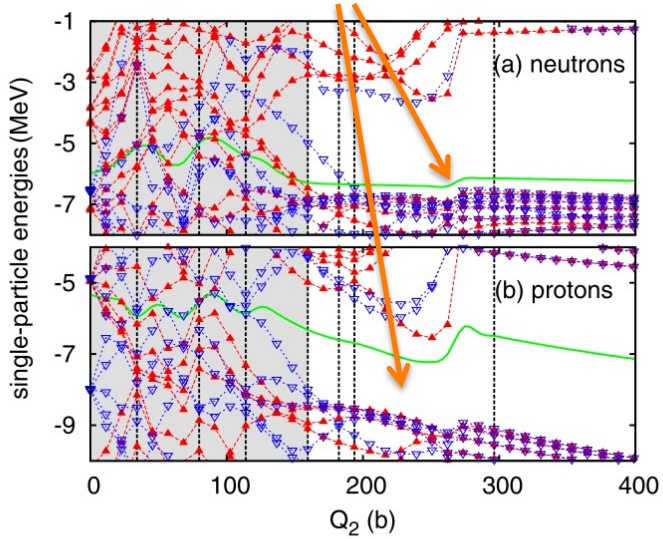

FIG. 2. (Color online) Single-particle energies in ^{258}Fm nucleus along the adiabatic PEC. The green solid curves show the neutron and proton Fermi energies. Positive and negative parity states are

From Tanimura, Lacroix, and Scamps,
Phys. Rev. C 92, 034601 (2015)

Main Theoretical Tool

THEOREM: There exist an universal density functional of particle density.

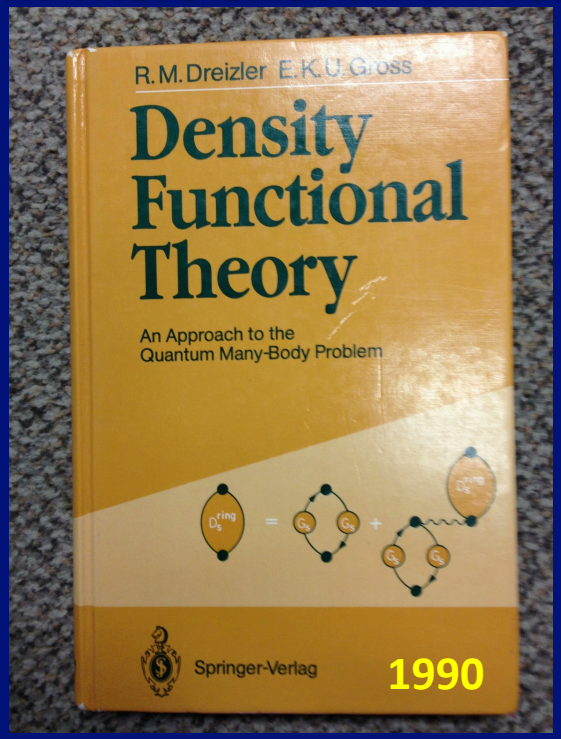

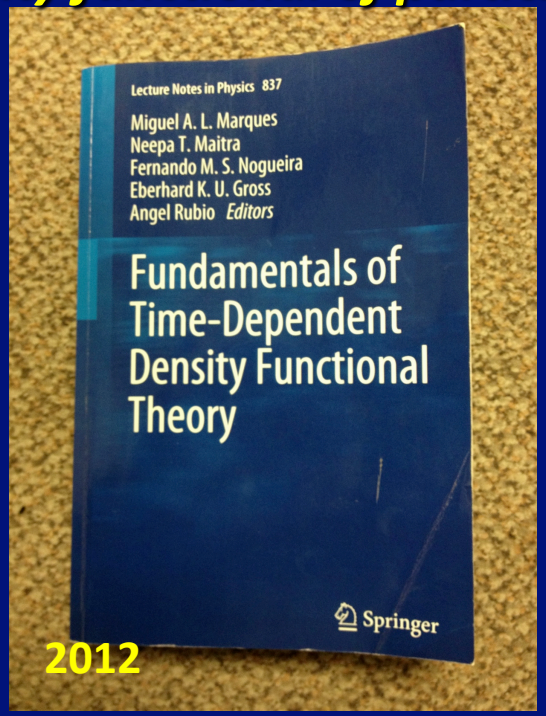

DFT has been developed and used mainly to describe normal (non-superfluid) electron systems – more than 50 years old theory:

DFT - Kohn and Hohenberg, 1964

LDA - Kohn and Sham, 1965

But not everyone is normal! Hence, a new local extension of DFT to superfluid systems and time-dependent phenomena was developed.

Review: A. Bulgac, *Time-Dependent Density Functional Theory and Real-Time Dynamics of Fermi Superfluids*, Ann. Rev. Nucl. Part. Sci. 63, 97 (2013)

Kohn-Sham theorem (1965)

$$H = \sum_{i}^{N} T(i) + \sum_{i<j}^{N} U(ij) + \sum_{i<j<k}^{N} U(ijk) + \ldots + \sum_{i}^{N} V_{ext}(i)$$

$$H\Psi_0(1,2,\ldots N) = E_0\Psi_0(1,2,\ldots N)$$

$$n(\vec{r}) = \left\langle \Psi_0 \left| \sum_{i}^{N} \delta(\vec{r} - \vec{r}_i) \right| \Psi_0 \right\rangle$$

Injective map (one-to-one)!

$$\Psi_0(1,2,\ldots N) \quad \Leftrightarrow \quad V_{ext}(\vec{r}) \quad \Leftrightarrow \quad n(\vec{r})$$

$$E_0 = \min_{n(\vec{r})} \int d^3r \left\{ \frac{\hbar^2}{2m^*(\vec{r})} \tau(\vec{r}) + \varepsilon\left[n(\vec{r}) \right] + V_{ext}(\vec{r}) n(\vec{r}) \right\}$$

$$n(\vec{r}) = \sum_{i}^{N} \left| \varphi_i(\vec{r}) \right|^2, \qquad \tau(\vec{r}) = \sum_{i}^{N} \left| \vec{\nabla} \varphi_i(\vec{r}) \right|^2$$

THEOREM: There exist an universal functional of particle density alone independent of the external potential.

The wave function of ^{240}Pu depends on 720 coordinates!!!
It has 1.76×10^{72} spin components!!!

SLDA Extension to Superfluids and Time-Dependent Phenomena, and Verification and Validation

- Since DFT/SLDA is not an approximation, but in principle an exact theoretical framework (unlike HF, HFB, etc.), one has to convincingly prove that its specific realization is equivalent to the Schrödinger equation! (The DFT and the Schrödinger descriptions should be identical.)

- Also, that it correctly describes Nature!

- And also, that the numerical implementation faithfully reproduces the theory.

There exists a real physical system, the Unitary Fermi Gas introduced by G.F. Bertsch, The Many-Body X Challenge, 1999 where many of these aspects can be directly verified:

The Unitary Fermi.

The SLDA energy density functional for unitary Fermi gas (infinite scattering length and zero effective range)

Dimensional arguments, renormalizability, Galilean invariance, and symmetries *determine fully the functional form of the energy density.*

In this respect this system is perhaps unique in Nature. It describes cold atoms and to a large extent dilute neutron matter, making it an ideal testing ground for DFT.

$$\varepsilon(\vec{r}) = \frac{\hbar^2}{m}\left\{\left[\alpha\frac{\tau_c(\vec{r})}{2} + \gamma\frac{\left|\nu_c(\vec{r})\right|^2}{n^{1/3}(\vec{r})}\right] + \beta\frac{3(3\pi^2)^{2/3}n^{5/3}(\vec{r})}{5}\right\} - \frac{\hbar^2}{m}(\alpha-1)\frac{\vec{j}^{\,2}(\vec{r})}{2n(\vec{r})}$$

$$n(\vec{r}) = 2\sum_{0<E_k<E_c}\left|\mathrm{v}_\mathrm{k}(\vec{r})\right|^2, \quad \tau_c(\vec{r}) = 2\sum_{0<E_k<E_c}\left|\vec{\nabla}\mathrm{v}_\mathrm{k}(\vec{r})\right|^2,$$

$$\nu_c(\vec{r}) = \sum_{0<E<E_c}\mathrm{u}_\mathrm{k}(\vec{r})\mathrm{v}_\mathrm{k}^*(\vec{r}) \quad \Leftarrow \text{ divergent without a cutoff, need RG}$$

- **Surprisingly, the gradient corrections are negligible!**
- **Three dimensionless constants α, β, and γ determining the functional are extracted from Quantum Monte Carlo for homogeneous systems and they determine the total energy, the pairing gap and the effective mass.**

Normal State				Superfluid State			
(N_a, N_b)	E_{FNDMC}	E_{ASLDA}	(error)	(N_a, N_b)	E_{FNDMC}	E_{ASLDA}	(error)
(3,1)	6.6 ± 0.01	6.687	1.3%	(1,1)	2.002 ± 0	2.302	15%
(4,1)	8.93 ± 0.01	8.962	0.36%	(2,2)	5.051 ± 0.009	5.405	7%
(5,1)	12.1 ± 0.1	12.22	0.97%	(3,3)	8.639 ± 0.03	8.939	3.5%
(5,2)	13.3 ± 0.1	13.54	1.8%	(4,4)	12.573 ± 0.03	12.63	0.48%
(6,1)	15.8 ± 0.1	15.65	0.93%	(5,5)	16.806 ± 0.04	16.19	3.7%
(7,2)	19.9 ± 0.1	20.11	1.1%	(6,6)	21.278 ± 0.05	21.13	0.69%
(7,3)	20.8 ± 0.1	21.23	2.1%	(7,7)	25.923 ± 0.05	25.31	2.4%
(7,4)	21.9 ± 0.1	22.42	2.4%	(8,8)	30.876 ± 0.06	30.49	1.2%
(8,1)	22.5 ± 0.1	22.53	0.14%	(9,9)	35.971 ± 0.07	34.87	3.1%
(9,1)	25.9 ± 0.1	25.97	0.27%	(10,10)	41.302 ± 0.08	40.54	1.8%
(9,2)	26.6 ± 0.1	26.73	0.5%	(11,11)	46.889 ± 0.09	45	4%
(9,3)	27.2 ± 0.1	27.55	1.3%	(12,12)	52.624 ± 0.2	51.23	2.7%
(9,5)	30 ± 0.1	30.77	2.6%	(13,13)	58.545 ± 0.18	56.25	3.9%
(10,1)	29.4 ± 0.1	29.41	0.034%	(14,14)	64.388 ± 0.31	62.52	2.9%
(10,2)	29.9 ± 0.1	30.05	0.52%	(15,15)	70.927 ± 0.3	68.72	3.1%
(10,6)	35 ± 0.1	35.93	2.7%	(1,0)	1.5 ± 0.0	1.5	0%
(20,1)	73.78 ± 0.01	73.83	0.061%	(2,1)	4.281 ± 0.004	4.417	3.2%
(20,4)	73.79 ± 0.01	74.01	0.3%	(3,2)	7.61 ± 0.01	7.602	0.1%
(20,10)	81.7 ± 0.1	82.57	1.1%	(4,3)	11.362 ± 0.02	11.31	0.49%
(20,20)	109.7 ± 0.1	113.8	3.7%	(7,6)	24.787 ± 0.09	24.04	3%
(35,4)	154 ± 0.1	154.1	0.078%	(11,10)	45.474 ± 0.15	43.98	3.3%
(35,10)	158.2 ± 0.1	158.6	0.27%	(15,14)	69.126 ± 0.31	62.55	9.5%
(35,20)	178.6 ± 0.1	180.4	1%				

Bulgac, Forbes, and Magierski, Ch.9 in Lecture Notes in Physics, vol. 836 (2012)

Formalism for Time-Dependent Phenomena

"The time-dependent density functional theory is viewed in general as a reformulation of the exact quantum mechanical time evolution of a many-body system when only one-body properties are considered."

A.K. Rajagopal and J. Callaway, Phys. Rev. B 7, 1912 (1973)
V. Peuckert, J. Phys. C 11, 4945 (1978)
E. Runge and E.K.U. Gross, Phys. Rev. Lett. 52, 997 (1984)

http://www.tddft.org

Time-Dependent Superfluid Local Density Approximation (TDSLDA)

$$E(t) = \int d^3r \left[\varepsilon(n(\vec{r},t), \tau(\vec{r},t), \nu(\vec{r},t), \vec{j}(\vec{r},t)) + V_{ext}(\vec{r},t) n(\vec{r},t) + \ldots \right]$$

$$\begin{cases} i\hbar \dfrac{\partial \mathrm{u}_i(\vec{r},t)}{\partial t} = [h(\vec{r},t) + V_{ext}(\vec{r},t) - \mu]\mathrm{u}_i(\vec{r},t) + [\Delta(\vec{r},t) + \Delta_{ext}(\vec{r},t)]\mathrm{v}_i(\vec{r},t) \\ i\hbar \dfrac{\partial \mathrm{v}_i(\vec{r},t)}{\partial t} = [\Delta^*(\vec{r},t) + \Delta^*_{ext}(\vec{r},t)]\mathrm{u}_i(\vec{r},t) - [h(\vec{r},t) + V_{ext}(\vec{r},t) - \mu]\mathrm{v}_i(\vec{r},t) \end{cases}$$

Galilean invariance determines the functional dependence on currents.

A great example on how TDSLDA help clarify a great puzzle and give a correct interpretation to an experimental result. The "heavy soliton" proved to be a vortex ring.

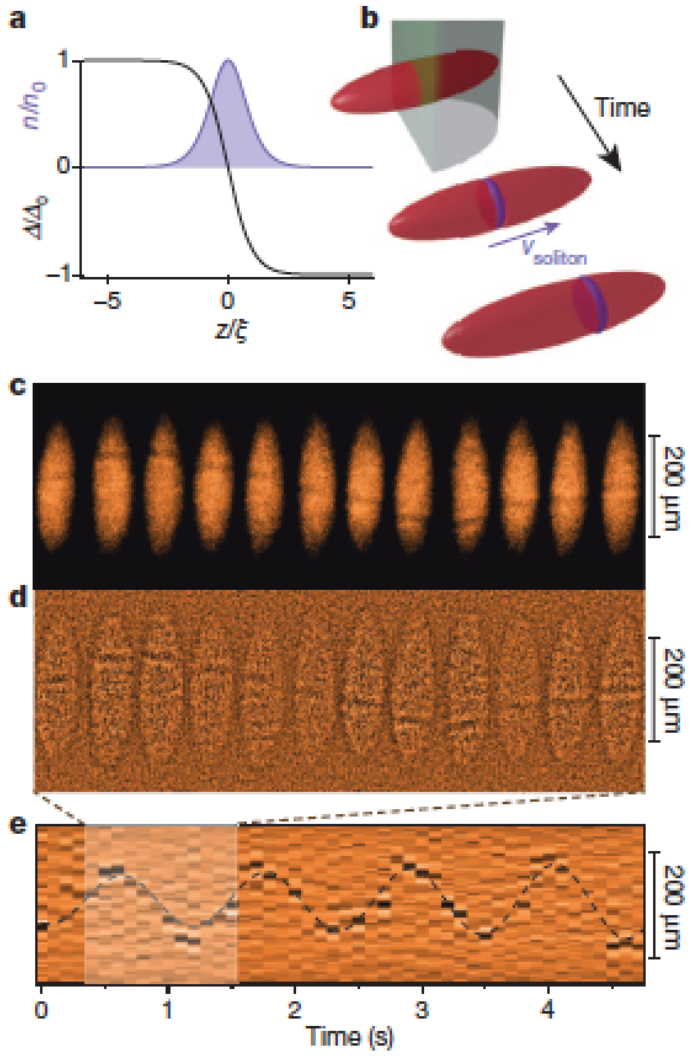

Heavy solitons in a fermionic superfluid

Tarik Yefsah[1], Ariel T. Sommer[1], Mark J. H. Ku[1], Lawrence W. Cheuk[1], Wenjie Ji[1], Waseem S. Bakr[1] & Martin W. Zwierlein[1]

Nature, 429, 426-430 (2013)

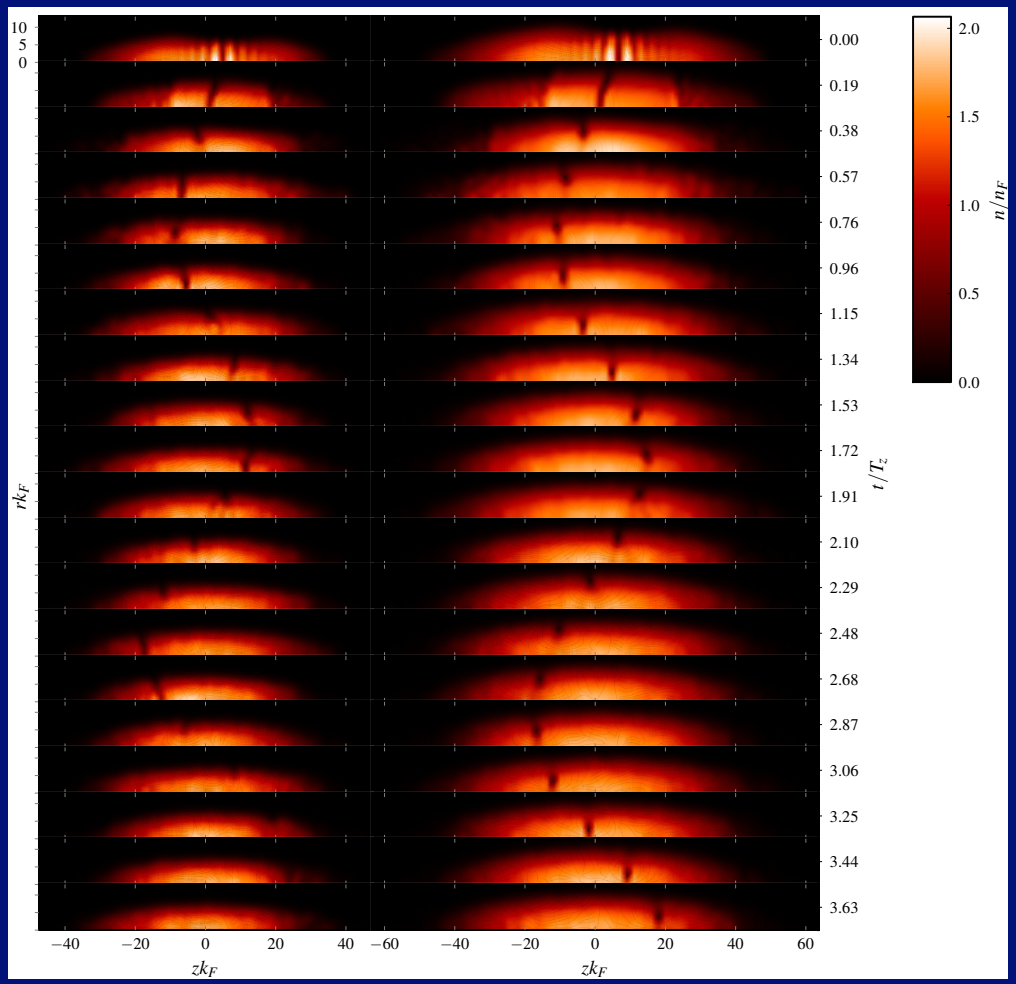

PRL 112, 025301 (2014) PHYSICAL REVIEW LETTERS week ending 17 JANUARY 2014

Quantized Superfluid Vortex Rings in the Unitary Fermi Gas

Aurel Bulgac,[1] Michael McNeil Forbes,[2,1,3] Michelle M. Kelley,[4] Kenneth J. Roche,[5,1] and Gabriel Wlazłowski[6,1]

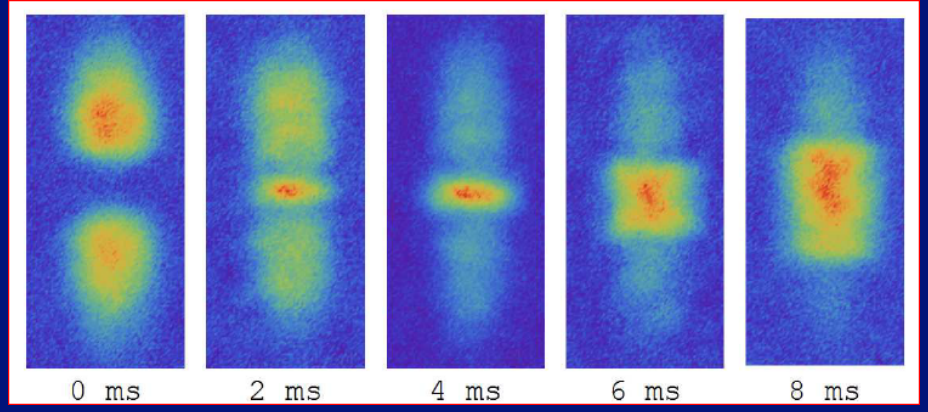

Observation of shock waves in a strongly interacting Fermi gas

J. Joseph, J.E. Thomas, M. Kulkarni, and A.G. Abanov Phys. Rev. Lett. 106, 150401 (2011)

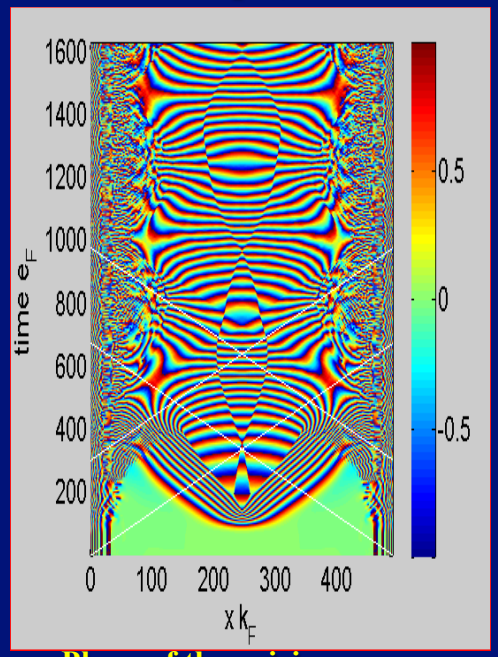

Phase of the pairing gap

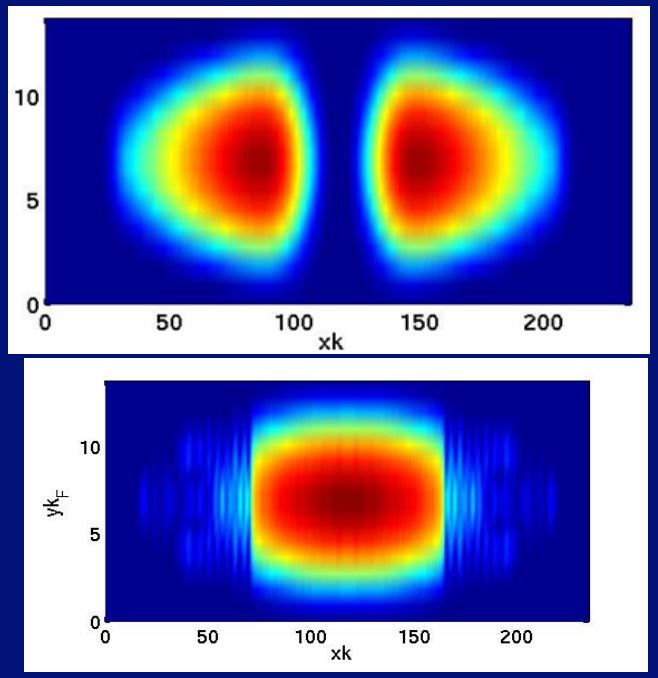

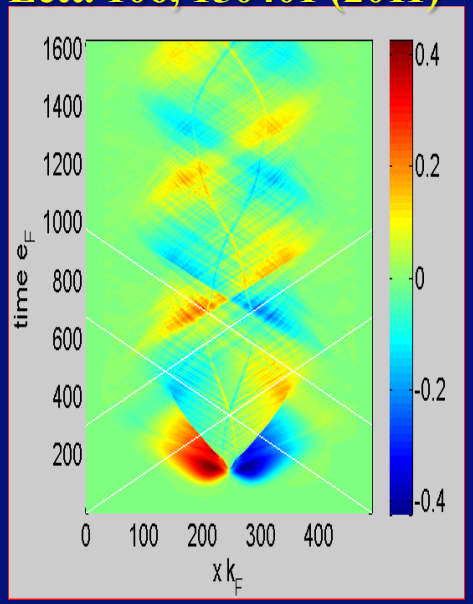

Local velocity normalized to Fermi velocity

Dark solitons/domain walls and shock waves in the collision of two UFG clouds of about 1,400 fermions, simulating a real experiment.

Bulgac, Luo, and Roche, Phys. Rev. Lett. 108, 150401 (2012)

The first ab initio simulation of quantum turbulence in a fermionic superfluid.

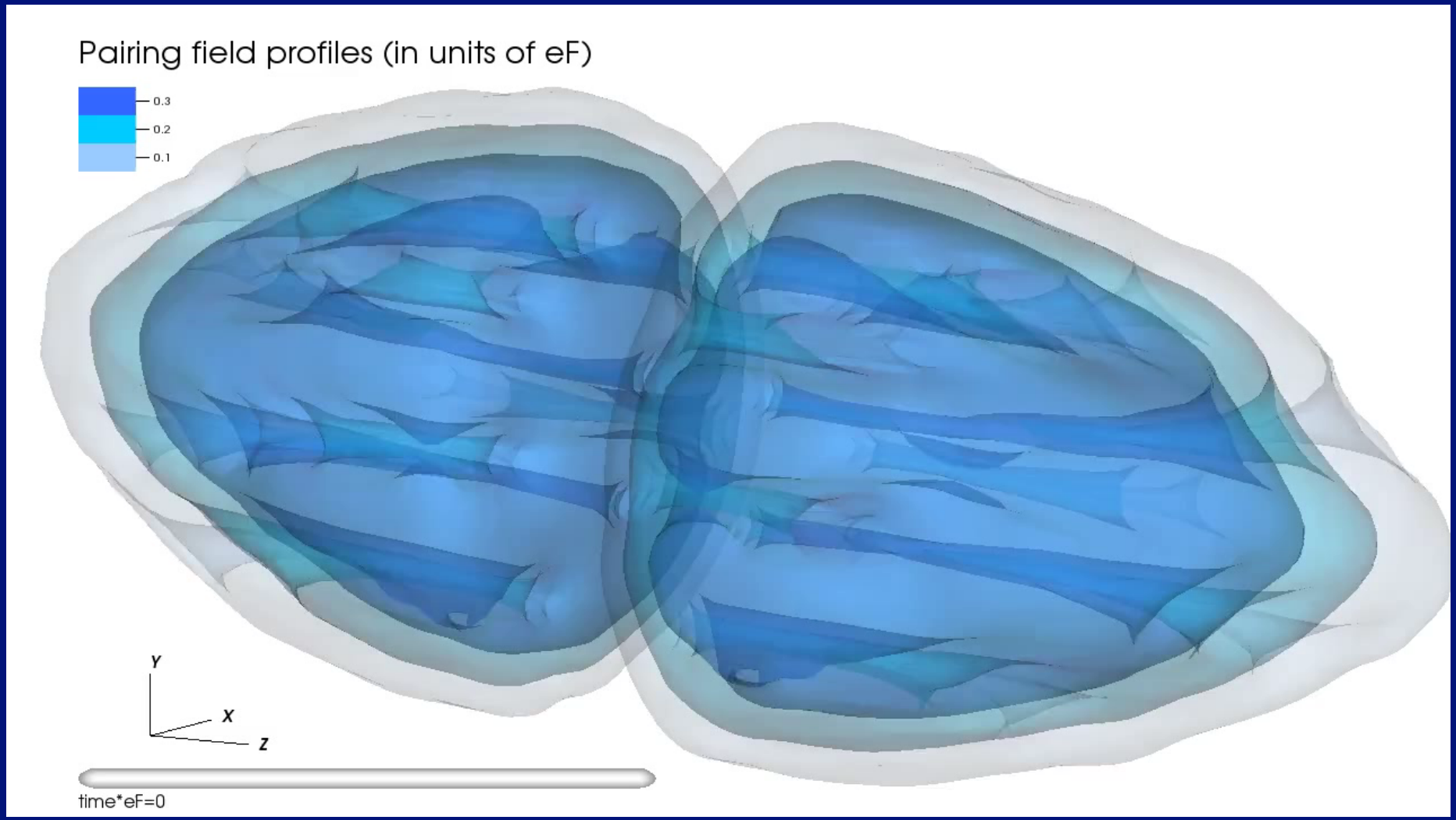

Aproximately 1270 fermions on a 48x48x128 spatial lattice, ≈ 260,000 complex PDEs, ≈ 309,000 time-steps, 2048 GPUs on Titan, 27.25 hours of wall time (initial code).

Wlazłowski et al, Phys. Rev. Lett. 112, 025301 (2014), Phys. Rev. A 91, 031602(R) (2015)

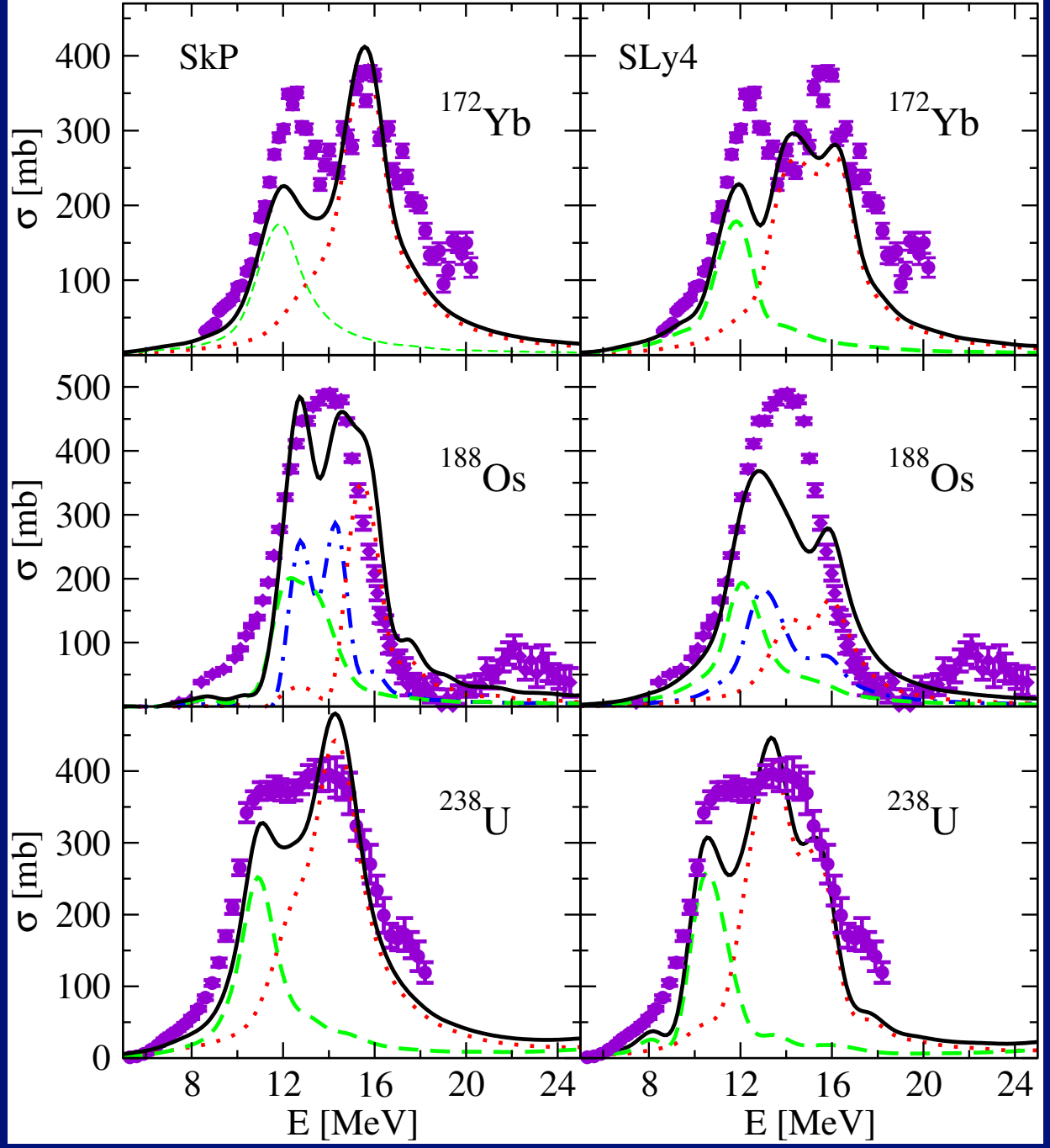

Giant Dipole Resonance deformed and superfluid Nuclei.

Osmium is triaxial, and both protons and neutrons are superfluid.

Stetcu, *et al.*, Phys. Rev. C 84, 051309(R) (2011)

Main computational tool

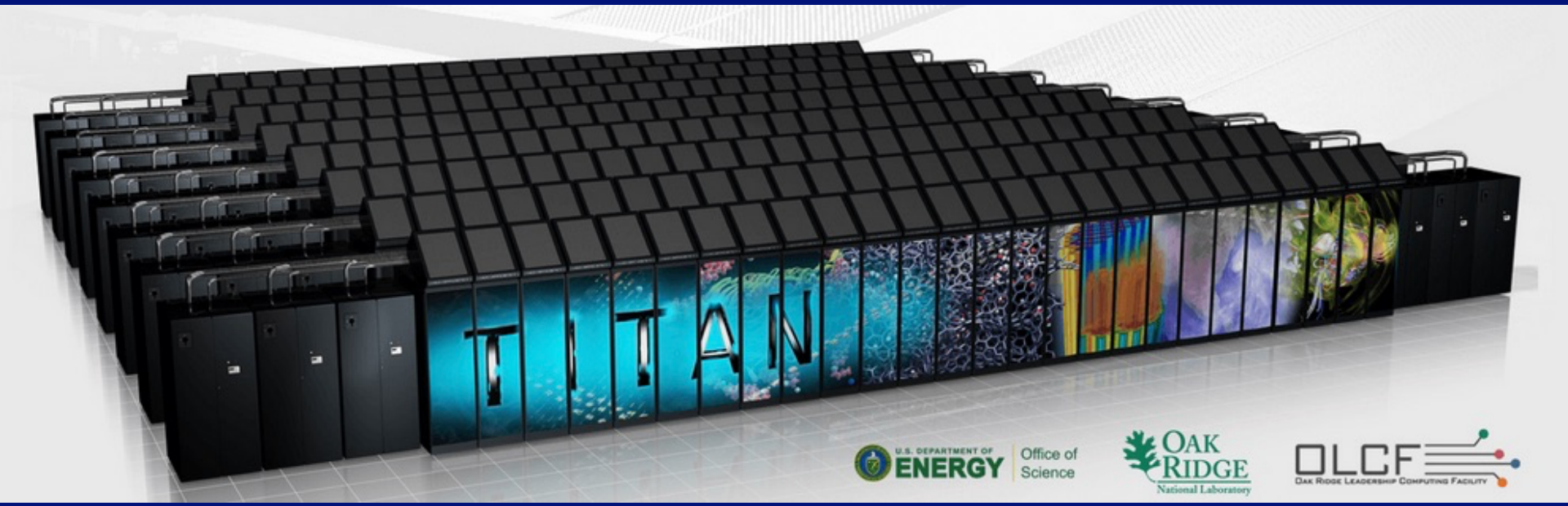

Cray XK7, ranked #2, at peak ≈ 27 Petaflops (Peta – 10^{15})

On Titan there are 18,688 GPUs , which provide 24.48 Petaflops !!!
and 299,008 CPUs which provide only 2.94 Petaflops

A single GPU on Titan performs the same amount of FLOPs as approximately 134 CPUs.

Bright future for GPU computing

US Department of Energy Supercomputers				
	Summit	**Titan**	**Sierra**	**Sequoia**
CPU Architecture	IBM POWER9	AMD Opteron (Bulldozer)	IBM POWER9	IBM BlueGene/Q
GPU Architecture	NVIDIA Volta	NVIDIA Kepler	NVIDIA Volta	N/A
Performance (RPEAK)	150 - 300 PFLOPS	27 PFLOPS	100+ PFLOPS	20 PFLOPS
Power Consumption	~10MW	~9MW	N/A	~8MW
Nodes	3,400	18,688	N/A	N/A
Laboratory	Oak Ridge	Oak Ridge	Lawrence Livermore	Lawrence Livermore
			IBM	IBM

Tesla Products	**Tesla K40**	**Tesla M40**	**Tesla P100**
GPU	GK110 (Kepler)	GM200 (Maxwell)	GP100 (Pascal)
SMs	15	24	56
TPCs	15	24	28
FP32 CUDA Cores / SM	192	128	64
FP32 CUDA Cores / GPU	2880	3072	3584
FP64 CUDA Cores / SM	64	4	32
FP64 CUDA Cores / GPU	960	96	1792
Base Clock	745 MHz	948 MHz	1328 MHz
GPU Boost Clock	810/875 MHz	1114 MHz	1480 MHz
Peak FP32 GFLOPs[1]	5040	6840	10600
Peak FP64 GFLOPs[1]	1680	210	5300
Texture Units	240	192	224
Memory Interface	384-bit GDDR5	384-bit GDDR5	4096-bit HBM2
Memory Size	Up to 12 GB	Up to 24 GB	16 GB
L2 Cache Size	1536 KB	3072 KB	4096 KB

Numerical Implementation and Deployment of TDSLDA on leadership class computers

TDSLDA equations

$$i\hbar\frac{\partial}{\partial t}\begin{pmatrix} u_{n\uparrow}(\vec{r},t) \\ u_{n\downarrow}(\vec{r},t) \\ v_{n\uparrow}(\vec{r},t) \\ v_{n\downarrow}(\vec{r},t) \end{pmatrix} = \begin{pmatrix} \hat{h}_{\uparrow\uparrow}(\vec{r},t)-\mu & \hat{h}_{\uparrow\downarrow}(\vec{r},t) & 0 & \Delta(\vec{r},t) \\ \hat{h}_{\downarrow\uparrow}(\vec{r},t) & \hat{h}_{\downarrow\downarrow}(\vec{r},t)-\mu & -\Delta(\vec{r},t) & 0 \\ 0 & -\Delta^*(\vec{r},t) & -\hat{h}^*_{\uparrow\uparrow}(\vec{r},t)+\mu & -\hat{h}^*_{\uparrow\downarrow}(\vec{r},t) \\ \Delta^*(\vec{r},t) & 0 & -\hat{h}^*_{\downarrow\uparrow}(\vec{r},t) & -\hat{h}^*_{\downarrow\downarrow}(\vec{r},t)+\mu \end{pmatrix} \begin{pmatrix} u_{n\uparrow}(\vec{r},t) \\ u_{n\downarrow}(\vec{r},t) \\ v_{n\uparrow}(\vec{r},t) \\ v_{n\downarrow}(\vec{r},t) \end{pmatrix}$$

- **The system is placed on a large 3D spatial lattice (adequate representation of continuum)**
- **Derivatives are computed with FFTW (this insures machine accuracy) and is very fast**
- **Fully self-consistent treatment with fundamental symmetries respected (isospin, gauge, Galilean, rotation, translation, parity)**
- **Adams-Bashforth-Milne fifth order predictor-corrector-modifier integrator Effectively a sixth order method**
- **No symmetry restrictions for the solutions**
- ***Number of PDEs is of the order of the number of spatial lattice points – from 10,000s to 1-2,000,000***

$$\propto 8\frac{4\pi p_c^3}{3}\left(\frac{L}{2\pi\hbar}\right)^3 \propto N_x N_y N_z$$

- **SLDA/TDSLDA (DFT) is formally by construction like meanfield HFB/BdG**
- **The code was implemented on Jaguar, Titan, Franklin, Hopper, Edison, Hyak, Athena**
- **Initially Fortran 90, 95, 2003 …, presently C, CUDA, and obviously MPI, threads, etc.**
- **Extremely efficient I/O for Check-Point Restart**
- **For more details about the method see INT talk on October 7, 2013:**

http://faculty.washington.edu/bulgac/talks.html#most_recent

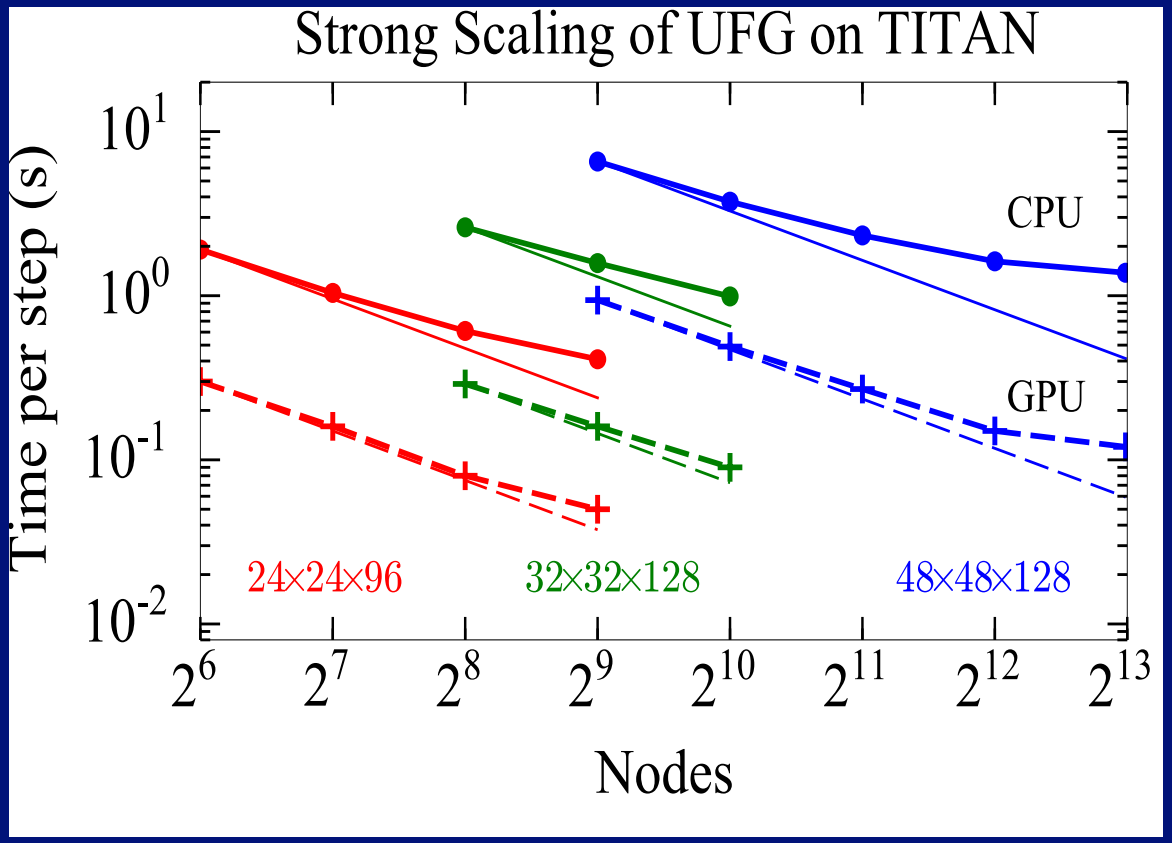

$N_xN_yN_z$	N_{wf}	memory	CPU comp. + comm.	CPU comp.	GPU comp. + comm.	GPU comp.	# of GPUs	speedup
48^3	110592	10 TB	3.9s	2.4s	0.39s	0.023s	6912	10
64^3	262144	56 TB	20s	9.1s	0.80s	0.48s	16384	25

Over 1 million time-dependent 3D nonlinear complex coupled PDEs

EDF : SLy4

Pairing coupling: $g_{\text{eff}}(\vec{r}) = g\left(1 - \eta \frac{\rho(\vec{r})}{\rho_0}\right)$

Simulation box: 40×22.5^2 fm^3

Momentum cutoff: $p_c = \frac{\hbar\pi}{\Delta x} = 500$ fm/c

Efficient use of FFT to calculate exactly derivatives

Adams-Bashforth-Milne O(Δt^6) time integration method

with only two evaluations of the rhs of the equations per time-step

Time-step: $= 0.119$ fm/c

Number of time steps: $\approx 120{,}000$

Number of PDEs: $\approx 56{,}000$

Number of GPUs: $\approx 1{,}750$

Wall time: $\approx$ 550 minutes

OLCF Titan - Cray XK7

Induced Fission of ^{240}Pu

- **No need to introduce and to guess the number and character of collective variables. The number of excited shape degrees of freedom is large and it increases during the evolution. This makes treatments like GCM, based on a fix number of collective coordinates quite doubtful.**

- **No need to evaluate the rather ill-defined potential energy surface.** ***Not clear how to choose the collective coordinates, how to choose the constraints, how to choose their number, and whether to require the nucleus to be cold or not.***

- **No need to determine the rather ill-defined inertia tensor.** ***Several prescriptions are used in literature.***

- **There is no need to invoke (or not) adiabaticity, since as a matter of fact the dynamical evolution is not close to equilibrium, at either zero or at a finite temperature. The evolution is truly a non-equilibrium one.**

- **One-body dissipation, the window and wall dissipation mechanisms are automatically incorporated into the theoretical framework.**

- **No modeling (except for the energy density functional, which so far is tested in completely unrelated conditions).**

- **All shapes are allowed and the nucleus chooses dynamically the path in the shape space, the forces acting on nucleons are determined by the nucleon distributions and velocities, and the nuclear system naturally and smoothly evolves into separated fission fragments.**

- **There is no need to introduce such concepts as "rupture," which is an un-natural concept in quantum mechanics, where everything is smooth, and no need to worry about how to define the scission configuration.**

- **One can extract difficult to gain otherwise information: angular momentum distribution and excitation energies of the fission fragments.**

Induced fission of ^{240}Pu

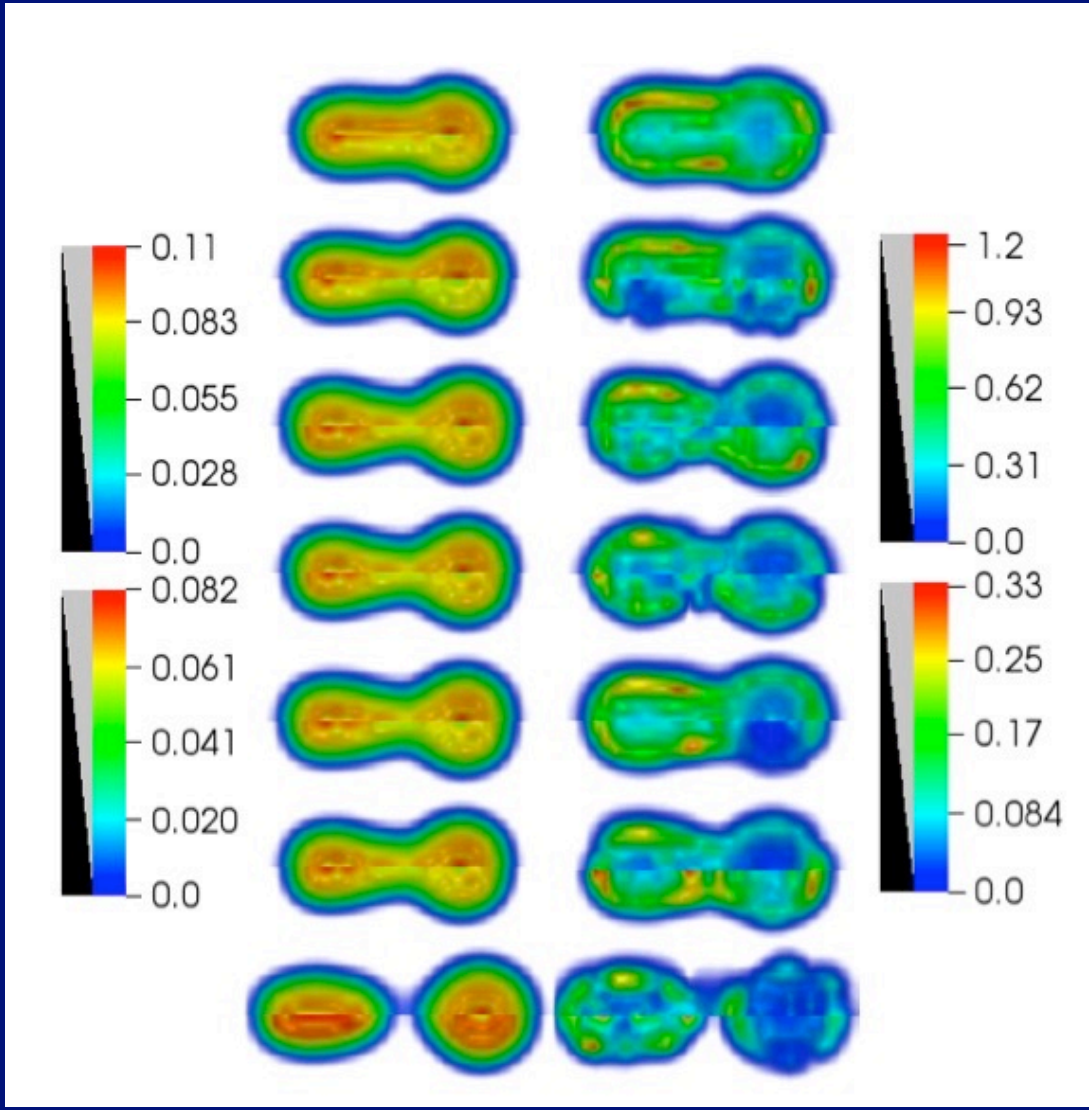

Neutron/proton densities (left and top/bottom)
Neutron/proton pairing gaps (right and top/bottom)

Bulgac, Magierski, Roche, and Stetcu, Phys. Rev. Lett. 116, 122504 (2016)

TABLE I. The simulation number, the pairing parameter η, the excitation energy (E^*) of $^{240}_{94}Pu_{146}$ and of the fission fragments [$E^*_{H,L} = E_{H,L}(t_{SS}) - E_{gs}(N_{H,L}, Z_{H,L})$], the equivalent neutron incident energy (E_n), the scaled initial mass moments $q_{20}(0)$ and $q_{30}(0)$, the "saddle-to-scission" time t_{SS}, TKE evaluated as in Ref. [71], TKE, atomic (A_L^{syst}), neutron (N_L^{syst}), and proton (Z_L^{syst}) extracted from data [72] using Wahl's charge systematics [73] and the corresponding numbers obtained in simulations, and the number of postscission neutrons for the heavy and light fragments ($\nu_{H,L}$), estimated using a Hauser-Feshbach approach and experimental neutron separation energies [8,74,75]. Units are in MeV, fm^2, fm^3, fm/c as appropriate.

S no.	η	E^*	E_n	q_{zz}	q_{zzz}	t_{SS}	TKE^{syst}	TKE	A_L^{syst}	A_L	N_L^{syst}	N_L	Z_L^{syst}	Z_L	E_H^*	E_L^*	ν_H	ν_L
$S1$	0.75	8.05	1.52	1.78	−0.742	14 419	177.27	182	100.55	104.0	61.10	62.8	39.45	41.2	5.26	17.78	0	1.9
$S2$	0.5	7.91	1.38	1.78	−0.737	4360	177.32	183	100.56	106.3	60.78	64.0	39.78	42.3	9.94	11.57	1	1
$S3$	0	8.08	1.55	1.78	−0.737	14 010	177.26	180	100.55	105.5	60.69	63.6	39.81	41.9	3.35	29.73	0	2.9
$S4$	0	6.17	−0.36	2.05	−0.956	12 751	177.92	181		103.9		62.6		41.3	7.85	9.59	1	1

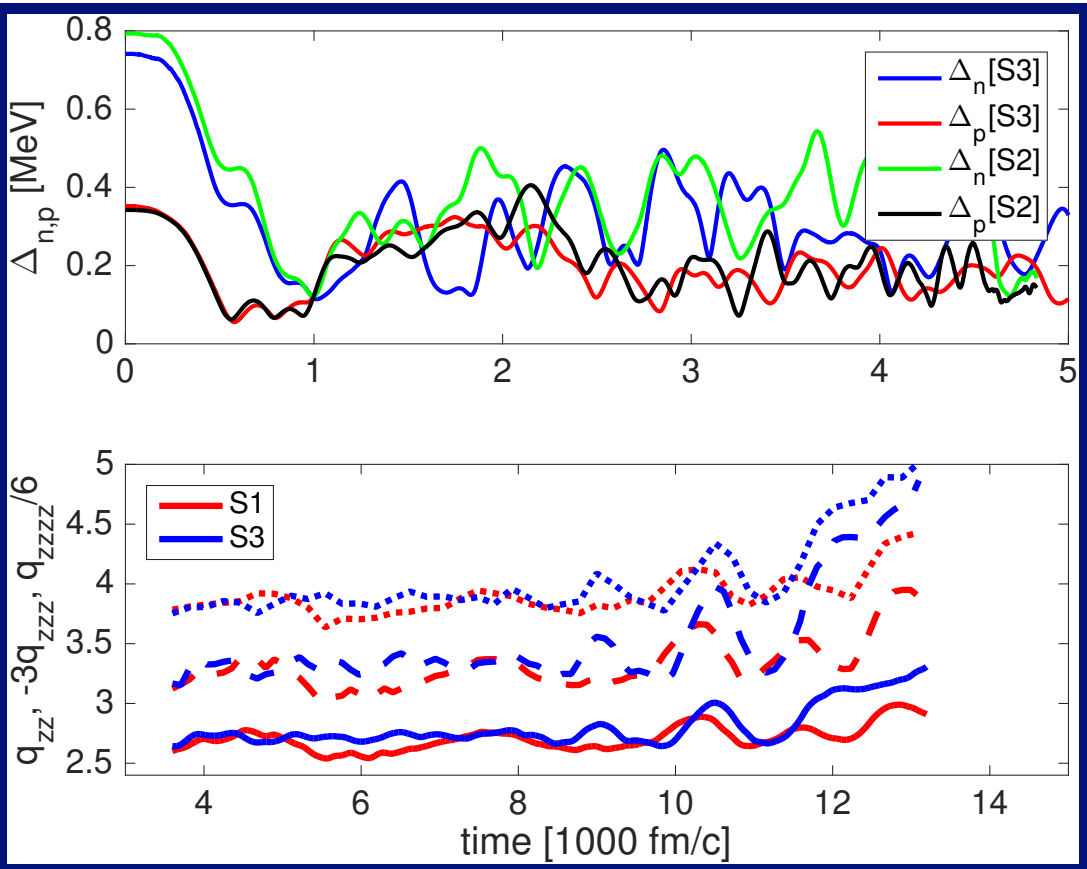

Evolution of the average magnitude of the pairing fields.

Hexadecapole (dashed), octupole (dotted), and quadrupole (solid) mass moments.

Fission of ^{240}Pu at excitation energy E_x = 8.08 MeV

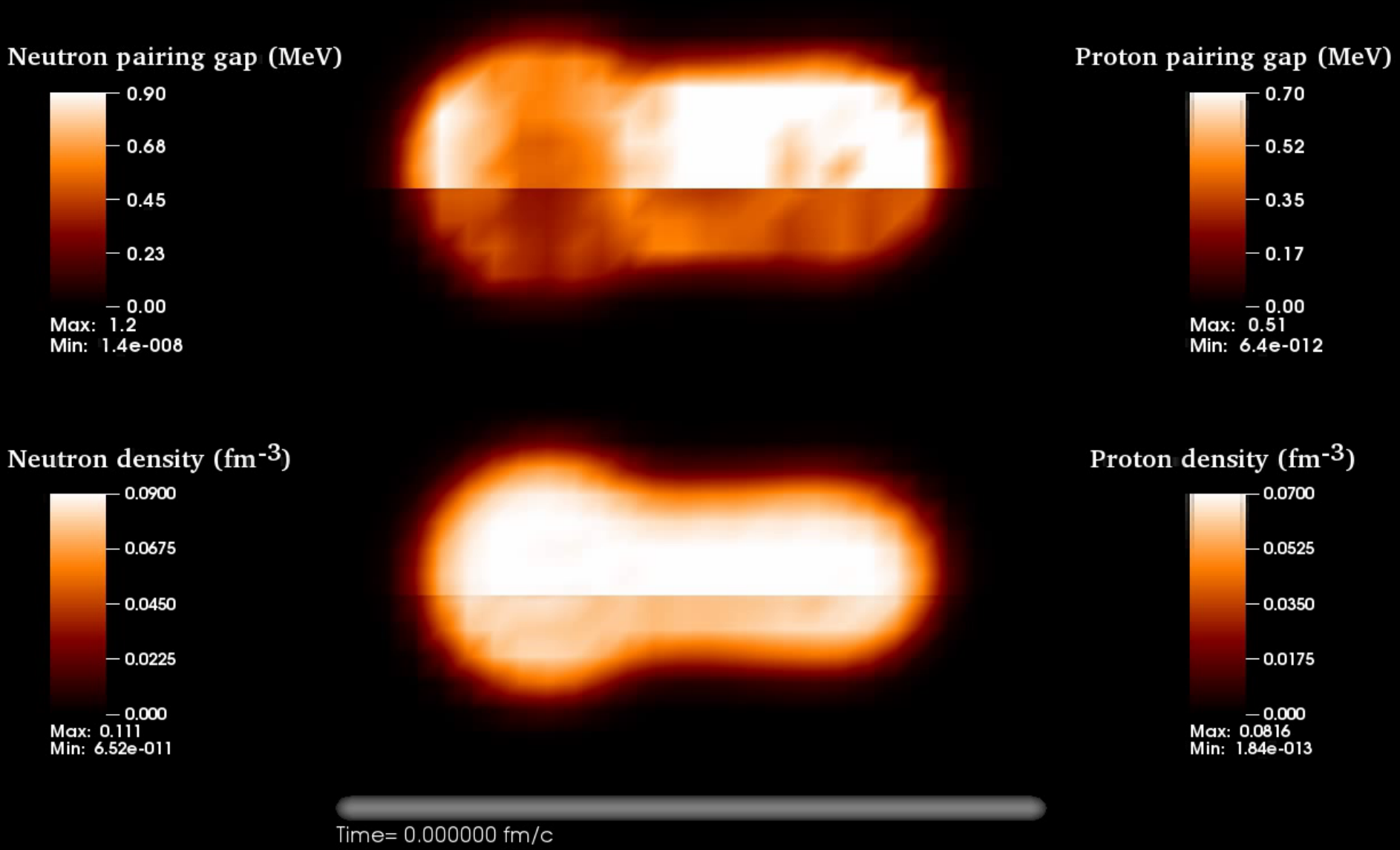

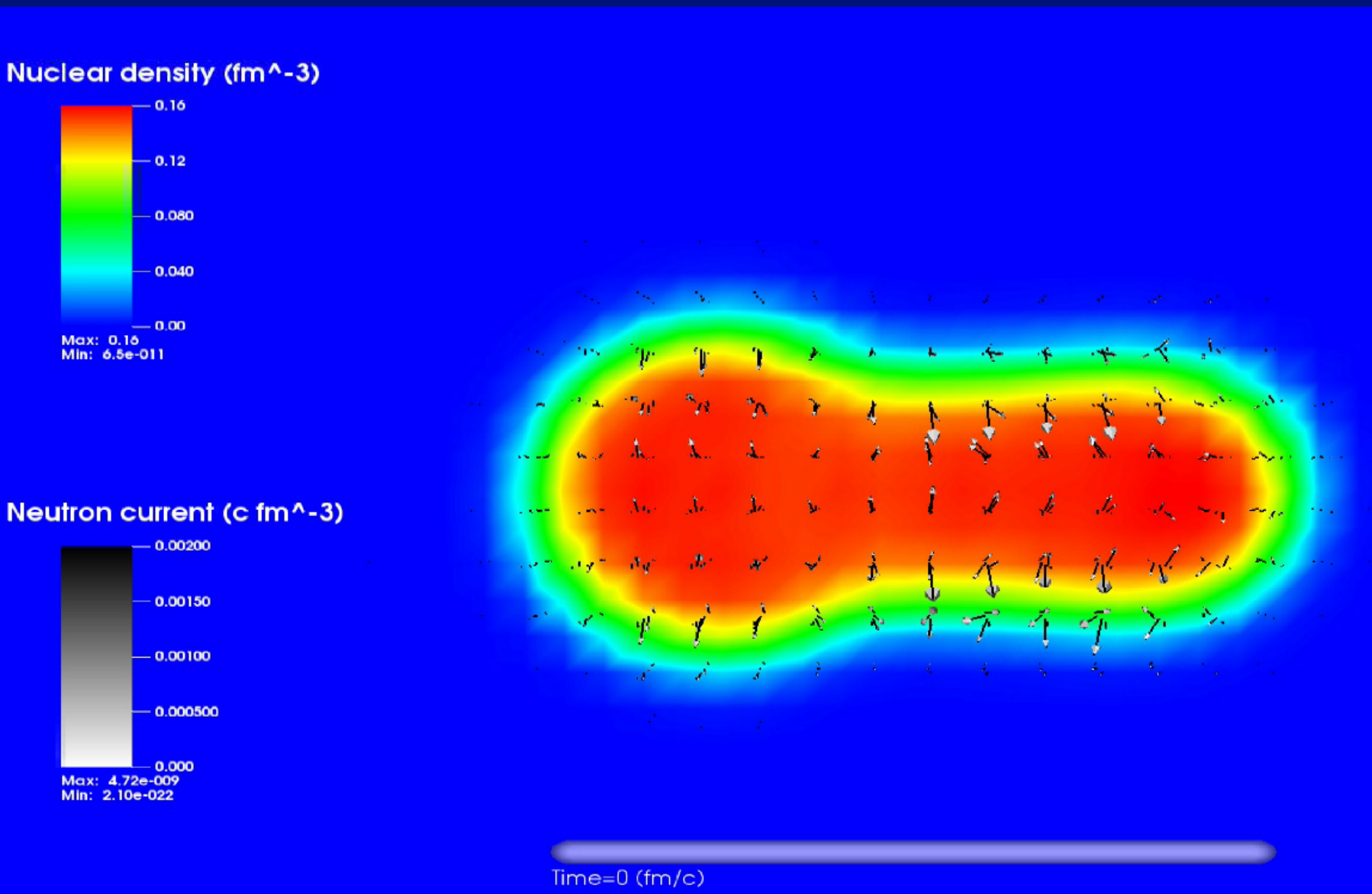
Nuclear density (fm^-3)
0.16
0.12
0.080
0.040
0.00
Max: 0.16
Min: 6.5e-011
Neutron current (c fm^-3)
0.00200
0.00150
0.00100
0.000500
0.000
Max: 4.72e-009
Min: 2.10e-022
Time=0 (fm/c)

Fission of ^{240}Pu at excitation energy E_x = 8.05; 7.91; 8.08 MeV

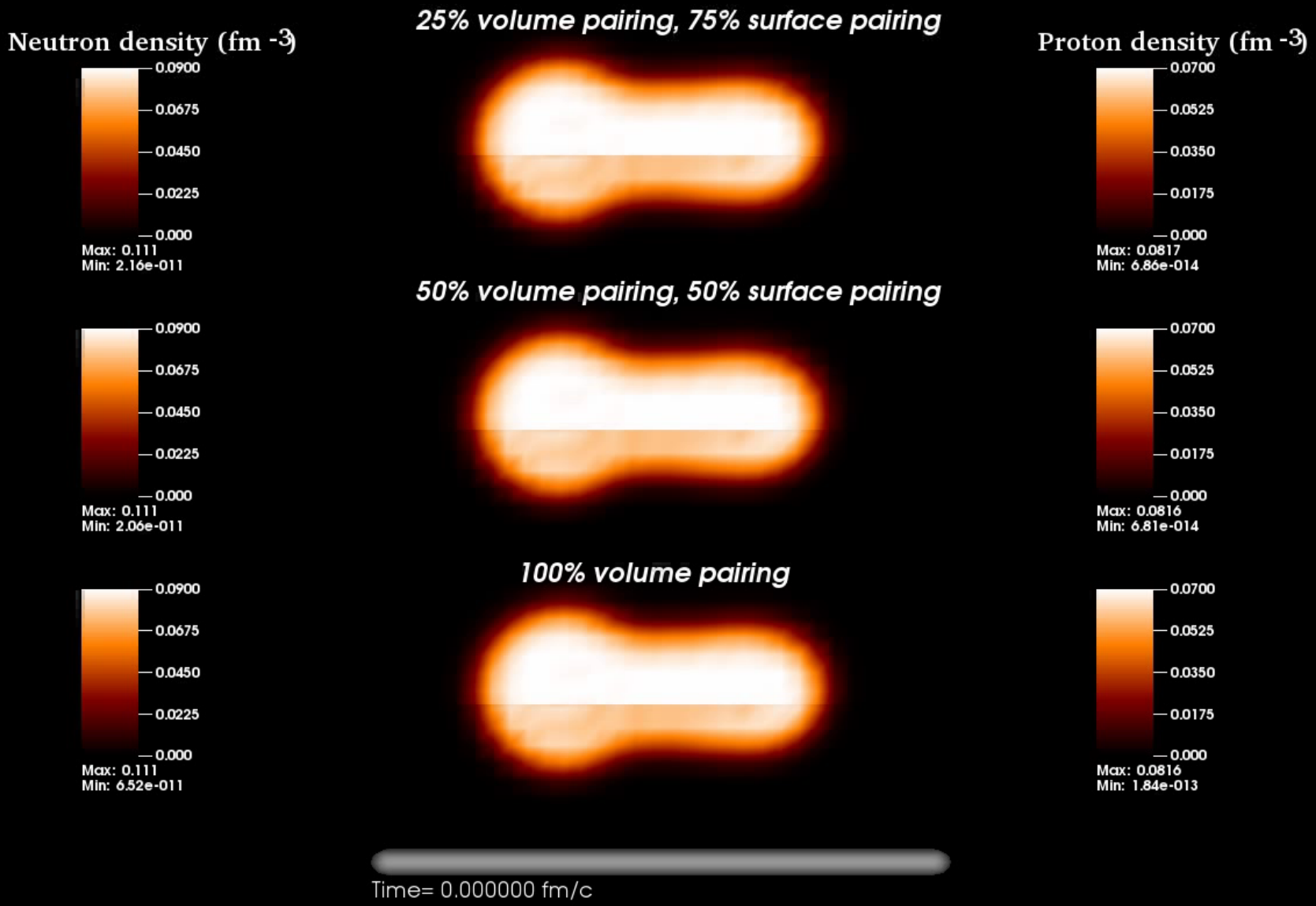

Fission of ^{240}Pu at excitation energy E_x = 8.05; 7.91; 8.08 MeV

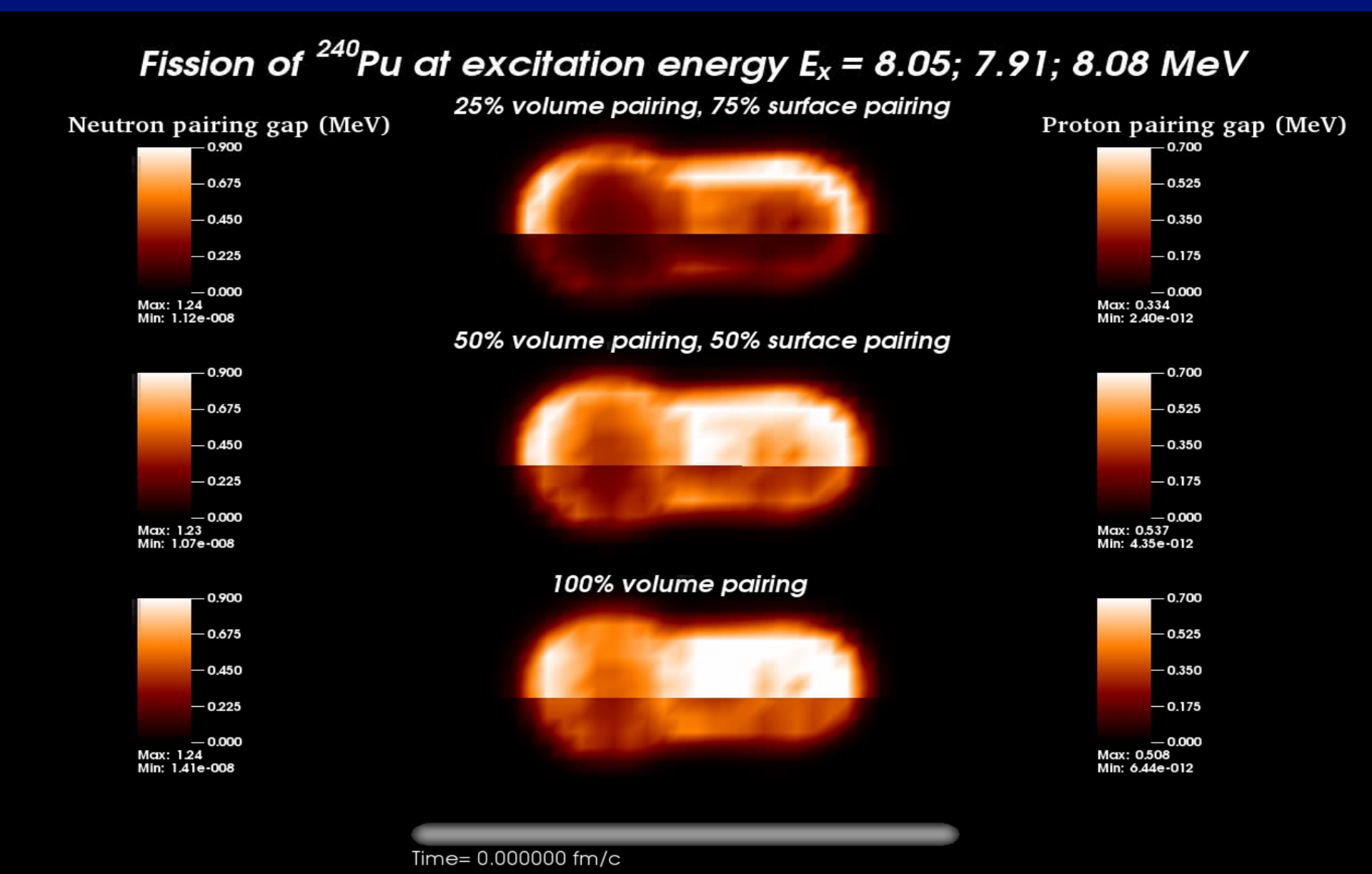

The most surprising finding was that the saddle-to-scission time was significantly longer than expected from any previous treatments.

Why?

The likeliest cause is the presence in TDSLDA of all possible collective degrees of freedom and that alone, even in the absence of dissipative effects results in longer saddle-to-scission times.

The fluctuating pairing filed, especially for protons, might also cause this behavior.

2D classical analog model of the Drude model for electron conduction in metals.

On the left side there is no "ion lattice" present, only electrons in an "uniform electric field."

On the right side the electrons, again in the presence of an "uniform electric field," collide elastically with the "ions."

Note that kinetic energy is not dissipated and in both cases and the "electrons" arrive at the bottom with the same speed but at different times!

Summary

- **TDSLDA will offer insights into nuclear processes and quantities which are either not easy or impossible to obtain in the laboratory:**

fission fragments excitation energies and angular momenta distributions,
element formation in astrophysical environments.
other nuclear reactions …

- **TDSLDA offers an unprecedented opportunity to test the nuclear energy density functional for large amplitude collective motion, non-equilibrium phenomena, and in new regions of the collective degrees of freedom.**

- **The quality of the agreement with experimental observations is surprisingly good, especially taking into account the fact that we made no effort to reproduce any measured data.**

- **TDSLDA predicts long saddle-to-scission time scales and the systems behaves superficially as a very viscous one, while at the same time the collective motion is not overdamped. There is no thermalization and the "temperatures" of the fission fragments are not equal.**

- **It is straightforward to implement the Balian and Vénéroni recipe to compute two-body observables: fission fragments mass, charge, angular momenta, excitation energy widths, …**

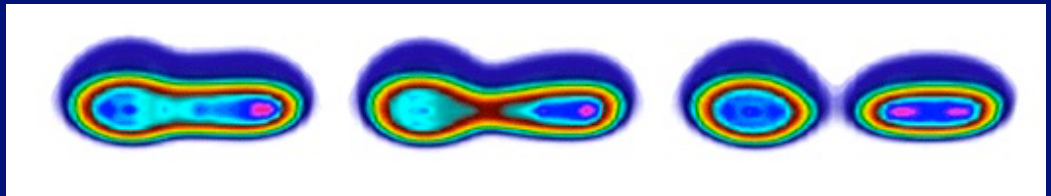

Papers we have published so far on SLDA and TDSLDA

Wlazłowski et al, Vortex pinning and dynamics, arxiv, to appear today
Phys. Rev. Lett. 116, 122504 (2016)
Phys. Rev. A 91, 031602(R) (2015)
Phys. Rev. Lett. 114, 012701 (2015)
Phys. Rev. Lett. 112, 025301 (2014)
arXiv:1305.6891
Phys. Rev. Lett. 110, 241102 (2013)
Phys. Rev. C 87 051301(R) (2013)
Ann. Rev. Nucl. Part. Phys. 63, 97 (2013)
Phys. Rev. Lett. 108, 150401 (2012)
Phys. Rev. C 84, 051309(R) (2011)
Science, 332, 1288 (2011)
J. Phys. G: Nucl. Phys. 37, 064006 (2010)
Phys. Rev. Lett. 102, 085302 (2009)
Phys. Rev. Lett. 101, 215301 (2008)
J.Phys. Conf. Ser. 125, 012064 (2008)
Chapter 9 in Lect. Notes Phys. vol. 836
Phys. Rev. A 76, 040502(R) (2007)
Int. J. Mod. Phys. E 13, 147 (2004)
Phys. Rev. Lett. 91, 190404 (2003)
Phys. Rev. Lett. 90, 222501 (2003)
Phys. Rev. Lett. 90, 161101 (2003)
Phys. Rev. C 65,051305(R) (2002)
Phys. Rev. Lett. 88, 042504 (2002)
Plus a few other chapters in various books.